

The structural connectivity of discrete networks underlies impulsivity and gambling in Parkinson's disease

Philip E. Mosley^{1,2,3,4,*} **Sae Paliwal**^{5,*} **Katherine Robinson**¹ **Terry Coyne**^{3,6} **Peter Silburn**^{2,3} **Marc Tittgemeyer**⁷ **Klaas E. Stephan**^{5,7,8} **Michael Breakspear**^{1,†} and **Alistair Perry**^{1,9,10,†}

*,[†]These authors contributed equally to this work.

See O'Callaghan (doi:10.1093/brain/awz349) for a scientific commentary on this article.

Impulsivity in Parkinson's disease may be mediated by faulty evaluation of rewards or the failure to inhibit inappropriate choices. Despite prior work suggesting that distinct neural networks underlie these cognitive operations, there has been little study of these networks in Parkinson's disease, and their relationship to inter-individual differences in impulsivity. High-resolution diffusion MRI data were acquired from 57 individuals with Parkinson's disease (19 females, mean age 62, mean Hoehn and Yahr stage 2.6) prior to surgery for deep brain stimulation. Reward evaluation and response inhibition networks were reconstructed with seed-based probabilistic tractography. Impulsivity was evaluated using two approaches: (i) neuropsychiatric instruments were used to assess latent constructs of impulsivity, including trait impulsiveness and compulsivity, disinhibition, and also impatience; and (ii) participants gambled in an ecologically-valid virtual casino to obtain a behavioural read-out of explorative, risk-taking, impulsive behaviour. Multivariate analyses revealed that different components of impulsivity were associated with distinct variations in structural connectivity, implicating both reward evaluation and response inhibition networks. Larger bet sizes in the virtual casino were associated with greater connectivity of the reward evaluation network, particularly bilateral fibre tracts between the ventral striatum and ventromedial prefrontal cortex. In contrast, weaker connectivity of the response inhibition network was associated with increased exploration of alternative slot machines in the virtual casino, with right-hemispheric tracts between the subthalamic nucleus and the pre-supplementary motor area contributing most strongly. Further, reduced connectivity of the reward evaluation network was associated with more 'double or nothing' gambles, weighted by connections between the subthalamic nucleus and ventromedial prefrontal cortex. Notably, the variance explained by structural connectivity was higher for behavioural indices of impulsivity, derived from clinician-administered tasks and the gambling paradigm, as compared to questionnaire data. Lastly, a clinically-meaningful distinction could be made amongst participants with a history of impulse control behaviours based on the interaction of their network connectivity with medication dosage and gambling behaviour. In summary, we report structural brain-behaviour covariation in Parkinson's disease with distinct reward evaluation and response inhibition networks that underlie dissociable aspects of impulsivity (*cf.* choosing and stopping). More broadly, our findings demonstrate the potential of using naturalistic paradigms and neuroimaging techniques in clinical settings to assist in the identification of those susceptible to harmful behaviours.

- 1 Systems Neuroscience Group, QIMR Berghofer Medical Research Institute, Herston, Queensland, Australia
- 2 Neurosciences Queensland, St Andrew's War Memorial Hospital, Spring Hill, Queensland, Australia
- 3 Queensland Brain Institute, University of Queensland, St Lucia, Queensland, Australia
- 4 Faculty of Medicine, University of Queensland, Herston, Queensland, Australia
- 5 Translational Neuromodeling Unit (TNU), Institute for Biomedical Engineering, University of Zürich and Swiss Federal Institute of Technology (ETH Zürich), Zürich, Switzerland

Received April 28, 2019. Revised July 25, 2019. Accepted August 30, 2019. Advance Access publication October 27, 2019

© The Author(s) (2019). Published by Oxford University Press on behalf of the Guarantors of Brain. All rights reserved.

For permissions, please email: journals.permissions@oup.com

- 6 Brizbrain and Spine, the Wesley Hospital, Auchenflower, Queensland, Australia
 7 Max Planck Institute for Metabolism Research, Cologne, Germany
 8 Wellcome Centre for Human Neuroimaging, University College London, London, UK
 9 Max Planck UCL Centre for Computational Psychiatry and Ageing Research, Berlin, Germany
 10 Centre for Lifespan Psychology, Max Planck Institute for Human Development, Berlin, Germany

Correspondence to: Dr Philip E. Mosley
 Neurosciences Queensland, Level 1, St Andrew's Place, 33 North Street, Spring Hill
 Queensland, 4000, Australia
 E-mail: philip.mosley@qimrberghofer.edu.au

Keywords: tractography; subthalamic nucleus; impulsivity; Parkinson's disease; gambling

Abbreviations: ACC = anterior cingulate cortex; BIS = Barratt Impulsiveness Scale; ELF = Excluded Letter Fluency task; ICB = impulse control behaviour; IFG = inferior frontal gyrus; LEDD = levodopa-equivalent daily dose; OFC = orbitofrontal cortex; PCA = principal components analysis; QUIP-RS = Questionnaire for Impulsive-Compulsive disorders in PD Rating Scale; SMA = supplementary motor area; STN = subthalamic nucleus; vmPFC = ventromedial prefrontal cortex; VS = ventral striatum; VTA = ventral tegmental area

Introduction

Parkinson's disease is generally viewed as a movement disorder characterized by slowing of action initiation, yet some individuals develop deficits in inhibitory-control and compulsive choice (Gauget *et al.*, 2004; Kobayakawa *et al.*, 2008; Milenkova *et al.*, 2011; Obeso *et al.*, 2011; Djamshidian *et al.*, 2012; Nombela *et al.*, 2014). Approximately 15% of those treated with dopamine replacement therapy develop a spectrum of impulse control behaviours (ICBs), including pathological gambling, hypersexuality, compulsive shopping and binge-eating (Weintraub *et al.*, 2010). However, other individuals with Parkinson's disease under the same treatment display no or less-pronounced impulsive biases without clinically-significant impairment, suggestive of underlying neurobiological differences in the susceptibility to ICBs. If these neurobiological determinants could be elucidated, enhanced identification of those vulnerable to ICBs would be possible. Furthermore, the understanding of other psychiatric conditions characterized by impulsivity and compulsivity (such as addiction) could be enriched (Robbins *et al.*, 2012).

Neurodegeneration and dopaminergic medication are two key biological mechanisms contributing to impulsivity in Parkinson's disease. Degeneration of midbrain dopaminergic neurons is the neuropathological hallmark of Parkinson's disease, most often affecting the ventral tier of neurons projecting to the dorsal striatum (Kish *et al.*, 1988), precipitating motor symptoms. However, the dorsal tier of neurons projecting to the ventral striatum (VS) (the mesolimbic pathway) may also be vulnerable to neurodegeneration, even at diagnosis (van der Vegt *et al.*, 2013). The VS is implicated in the integration of emotional, contextual and motivational information, with the ability to influence goal-oriented motor behaviour through feed-forward connections in the basal ganglia. For example, the VS is active during the experience of reward, and also during the anticipation of an appetitive stimulus, forming the basis of a reward prediction

error signal (Knutson *et al.*, 2001; O'Doherty *et al.*, 2002). Dopaminergic replacement therapy restores motor function in Parkinson's disease but may disrupt the homeostatic role of midbrain dopaminergic neurons and modulate the regulatory input of the prefrontal cortex to the VS (Goto and Grace, 2005; Grace, 2008). The preservation of mesolimbic relative to nigrostriatal projections in Parkinson's disease (Kumakura *et al.*, 2010) means that dopaminergic transients in the VS encoding reward prediction errors may be biased by supplemental dopaminergic medication and result in exaggerated 'better than expected' teaching signals, driving escalation of risky behaviours with a tendency to discount losses (Voon *et al.*, 2010a). Dopamine agonist medication also mediates elevated rates of reflection impulsivity (Djamshidian *et al.*, 2013), but only increases temporal discounting (Voon *et al.*, 2010b) and risk taking (Claassen *et al.*, 2011; Voon *et al.*, 2011) in individuals with pre-existing ICBs. This suggests that dopaminergic medication in Parkinson's disease is acting upon an 'at-risk' neural substrate rather than being a sufficient aetiological factor in isolation.

Reward evaluation and response inhibition are two distinct neurocognitive mechanisms that likely underlie impulsive behaviour (*cf.* making a choice versus suppressing an inappropriate choice). As aforementioned, reward evaluation (including appetitive learning and reinforcement) is underpinned by dopaminergic signalling within mesocorticolimbic networks (Haber and Knutson, 2010) and their connections with the orbitofrontal cortex (van Eimeren *et al.*, 2010) and anterior cingulate cortex (Cilia *et al.*, 2011; Carriere *et al.*, 2015). These cortical regions are associated with the prediction and evaluation of behavioural outcomes, amongst other functions (Rudebeck and Murray, 2014; Kolling *et al.*, 2016). Response inhibition is likely to be subserved by distinct neural networks in Parkinson's disease (Antonelli *et al.*, 2014) and healthy controls (Hampton *et al.*, 2017). This 'stopping network' has been well characterized in non-clinical populations and is a predominantly right-lateralized network involving the

inferior frontal gyrus (IFG), the pre-supplementary motor area (pre-SMA) and the subthalamic nucleus (STN) (Aron *et al.*, 2007; Rae *et al.*, 2015). The STN receives direct cortical projections from the IFG and pre-SMA in the ‘hyper-direct’ pathway, which serves to deliver a global ‘stopping’ signal to the basal ganglia in response to the detection of cognitive conflict (Aron, 2011). In Parkinson’s disease, the firing pattern of the STN increases in response to dopaminergic denervation (Vila *et al.*, 2000), leading to bradykinesia, rigidity and tremor that can be successfully treated with deep brain stimulation (DBS) (Schuepbach *et al.*, 2013), signifying the central role of this nucleus in the pathophysiology of motor symptoms. However, the spread of electrical stimulation throughout discrete territories of the topographically-organized STN may underlie increased impulsivity subsequent to STN-DBS (Mosley *et al.*, 2018b), supporting the role of this nucleus as a key node in non-motor aspects of response inhibition.

Diffusion MRI is a neuroimaging technique that can be used to characterize the architecture of white matter tracts in the brain (Jbabdi *et al.*, 2015), which may provide new insights into mechanisms of disease or therapy. For example, in Parkinson’s disease, the use of diffusion MRI has revealed that structural connectivity of motor networks is predictive of clinically-effective subthalamic stimulation (Accolla *et al.*, 2016; Vanegas-Aroyave *et al.*, 2016; Akram *et al.*, 2017; Horn *et al.*, 2017; Chen *et al.*, 2018). However, there has been little study of cortico-subcortical networks with reference to impulsivity in Parkinson’s disease, although spatially-extensive white matter pathology in frontostriatal circuits may be present at early clinical stages (Rae *et al.*, 2012). The presence of ICBs in Parkinson’s disease has been associated with reductions in diffusion tensor imaging (DTI)-derived indices of white matter ‘integrity’ within frontal and mesolimbic tracts (relative to non-ICB patients) (Imperiale *et al.*, 2018). However, these investigations are typically constrained to between-group comparisons (i.e. ICB versus non-ICBs), and hence the complex relationships between white matter changes and the multifaceted aspects of impulsivity remain poorly understood.

Using a high-resolution diffusion MRI acquisition, we sought to characterize the anatomical networks that underlie the different facets of impulsivity in Parkinson’s disease. We used neuropsychiatric instruments and a novel task assessing gambling behaviour (Paliwal *et al.*, 2019), which we hypothesized would form a more ecologically-valid measure of impulsivity. We postulated that dimensional variations in impulsivity would relate to interindividual differences in network connectivity, and that different networks would be implicated in different aspects of impulsive responding. By elucidating the multifaceted nature of impulsivity, spanning neuroanatomy and behaviour, during an ecologically-valid task, we aimed to create a behavioural read-out of impulsivity in Parkinson’s disease that could assist with diagnostic and prognostic assessment. In particular, we were interested in whether these measures would allow us to discriminate individuals with clinically-significant ICBs.

Materials and methods

Participants

Participants were consecutively recruited at the Asia-Pacific Centre for Neuromodulation in Brisbane, Australia between 2016 and 2018. All participants met the UK Brain Bank criteria for Parkinson’s disease (Hughes *et al.*, 1992) and at the time of recruitment were being assessed for STN-DBS. All participants were at Hoehn and Yahr stage 2 or greater (Hoehn and Yahr, 1967) with motor fluctuations or other motor complications related to dopaminergic therapy. No participants met the Movement Disorder Society criteria for dementia (Emre *et al.*, 2007). The disease subtype was established based on an analysis of the dominant symptoms elicited during the Unified Parkinson’s Disease Rating Scale (UPDRS) Part III Motor Examination, as described in Spiegel *et al.* (2007). Dopaminergic medication was converted to a levodopa-equivalent daily dose (LEDD) value (Evans *et al.*, 2004). Further details regarding recruitment and baseline assessment have been previously reported (Mosley *et al.*, 2018a).

Ethics approval

Prior to the commencement of data collection, the full protocol was approved by the Human Research Ethics Committees of the Royal Brisbane and Women’s Hospital, the University of Queensland, the QIMR Berghofer Medical Research Institute and UnitingCare Health. All participants gave written, informed consent to participate in the study.

Assessment of impulsivity

Neuropsychiatric instruments

Impulsivity was first assessed with a range of neuropsychiatric instruments, acknowledging the multidimensional nature of this construct. These included: trait impulsiveness: the Barratt Impulsiveness Scale 11 (BIS) and attentional, motor and non-planning subscales (Patton *et al.*, 1995); ICBs: the Questionnaire for Impulsive-Compulsive disorders in PD Rating Scale (QUIP-RS) (Weintraub *et al.*, 2012); impatience: the Delay Discounting task (Kirby *et al.*, 1999); disinhibition: the Excluded Letter Fluency task (ELF) (Shores *et al.*, 2006) and the Hayling test (Burgess *et al.*, 1997). Broadly, these instruments could be distinguished by modality: the BIS and QUIP-RS are questionnaires completed by the participant, whilst the ELF, Hayling and Delay Discounting tasks are administered by an examiner. Although the use of subscales has been criticized (Reise *et al.*, 2013), we opted to use the BIS subscales based on their prior utility in explicating relevant behavioural features of Parkinson’s disease (Antonini *et al.*, 2011; Smulders *et al.*, 2014) and in order to maintain consistency with prior work (Mosley *et al.*, 2018a). For further information see the Supplementary material.

Gambling paradigm

In addition to these classical assessments of impulsivity, participants also gambled on slot machines within a virtual casino, which has been described and validated in healthy

controls and individuals with Parkinson's disease (Paliwal *et al.*, 2014, 2019). The motivation for this task was to provide a realistic simulation of impulsive behaviours. Participants began the casino with 2000 AUD (virtual money) in their account, and played through 100 trials where a gambling choice was required. In the casino, there were four slot machines to choose from; participants could move between machines at any time. Each slot machine had a unique visual appearance and soundtrack and participants were informed that different machines might have different outcome expectancies. On each trial, participants placed a bet that they were able to increase in increments of 5 or 10 AUD with no maximum upper limit per bet. Once the bet was placed, a 'Pull!' button triggered three spinning wheels. After 5 s, the outcomes of the first, the second and third wheel were sequentially revealed. During this time, participants were also able to trigger an earlier reveal by using a 'Stop!' button. Win trials were signified by the nature of matching symbols across the three wheels. On all win trials, the participant was given the option to 'Double-Up!', engaging in a secondary double-or-nothing gamble, risking the total win amount (Supplementary Fig. 1). Notably, the trajectory of win-loss outcomes was predetermined, ensuring that participants' experience of rewards and losses were comparable in order and quantity. The trajectory resulted in a positive outcome (net winnings) for most participants. At the end of the task, participants were awarded up to 30 AUD in real money based on the size of these virtual winnings.

This naturalistic gambling task allowed for impulsive behaviour to be expressed in several ways on each trial: bet increases (in principle, of unlimited magnitude), exploratory slot machine switches, 'double or nothing' gambles and cash outs. Keeping in mind that in the behavioural sciences 'risk' is typically defined in relation to the variance of choice outcomes (Johnson and Busemeyer, 2010), these actions are indicative of exploration and risk-taking as they increase the range of possible outcomes. For example, for a machine switch, regardless of whether the player is performing well or poorly on the current machine, the decision to switch machines incurs the possibility that the new machine chosen may be more punishing or rewarding than the current machine, thereby making the player vulnerable to increased variance in outcomes. Similarly, a bet increase is a risk-inducing shift in the face of uncertainty, making the player more susceptible to larger wins and losses. In sum, each action implies a broadening of possible outcomes (risk), and may be understood as reflecting impulsivity.

A further description of the gambling paradigm can be found in Paliwal *et al.* (2019) and in the Supplementary material.

Participants completed the experimental tasks ON medication to protect participants against discomfort arising from OFF states, which were generally severe in this peri-surgical population. LEDD was included as a covariate in subsequent analyses. Although dopamine agonists as a class are associated with an elevated risk of ICBs (Weintraub *et al.*, 2010), we included all dopaminergic medication in the calculation of LEDD, given that ICBs are also more prevalent in individuals on levodopa, as well as the substantial prior literature linking dopamine to changes in reward learning (and thus impulsivity) in preclinical models (Schultz *et al.*, 1997), healthy individuals (Abler *et al.*, 2006) and individuals with Parkinson's disease (Frank *et al.*, 2004).

Diffusion-weighted imaging acquisition and preprocessing

Diffusion-weighted imaging (DWI) data were acquired along 90 directions using a 3 T Siemens PRISMA scanner and a 64-channel array head coil (b -value = 3000 s/mm², voxel size = 1.7 mm³ isotropic). Twelve non-diffusion-weighted images (b_0) were acquired and interleaved throughout this main sequence, while an additional sequence of eight b_0 images were also collected with the opposite phase-encoding (posterior-anterior) direction. A structural T₁-weighted MPRAGE (1-mm³ resolution) image was also acquired.

The DWI data were preprocessed with MRtrix3 software (Tournier *et al.*, 2019) (https://github.com/MRtrix3/mrtrix3/releases/tag/3.0_RC3), using an in-house preprocessing pipeline (<https://github.com/breakspear/diffusion-pipeline>). Preprocessing steps included denoising (Veraart *et al.*, 2016) and correction for motion, susceptibility, and eddy-current induced distortions (Andersson and Sotiropoulos, 2016). Finally, bias-intensity correction was performed (Zhang *et al.*, 2001; Smith *et al.*, 2004) (Fig. 1A). Full details on the DWI acquisition, preprocessing and fibre reconstruction steps are provided in the Supplementary material.

Fibre reconstruction, tractography, and apparent fibre density

To permit within-group comparisons of structural connectivity estimates, group-average intensity normalization was undertaken (Raffelt *et al.*, 2012), ensuring that the median b_0 white-matter value was uniform across study participants (Fig. 1B). From these data, constrained spherical deconvolution (CSD) (Tournier *et al.*, 2004, 2007; Jeurissen *et al.*, 2014) was performed in each participant (Fig. 1C), providing local (i.e. voxel-wise) estimates of fibre orientation distribution functions (fODF).

The probabilistic streamline algorithm iFOD2 (Tournier *et al.*, 2010) was used to reconstruct fibre-bundles between seed and target regions within two networks (defined *a priori*), with regions selected because of their involvement in reward evaluation and response inhibition (see below). Through sampling of the fODF at each path point, 100 streamlines were reconstructed (Fig. 1D).

Estimates of structural connectivity between each seed and target region were derived from the apparent fibre density representing the underlying intra-axonal volume (Raffelt *et al.*, 2012). For each pathway of interest, the apparent fibre density was calculated by summing the fODF lobe integrals, approximating the total fibre volume, and was then divided by the mean streamline length (Fig. 1E).

Reward evaluation and response inhibition networks

Two discrete brain networks subserving reward evaluation and response inhibition were reconstructed with seed-based tractography (Fig. 1F and G). The reward evaluation network (Fig. 1F) included streamline propagations connecting the VS with the ventromedial prefrontal cortex (vmPFC), the orbitofrontal cortex (OFC), the anterior cingulate cortex (ACC) and the

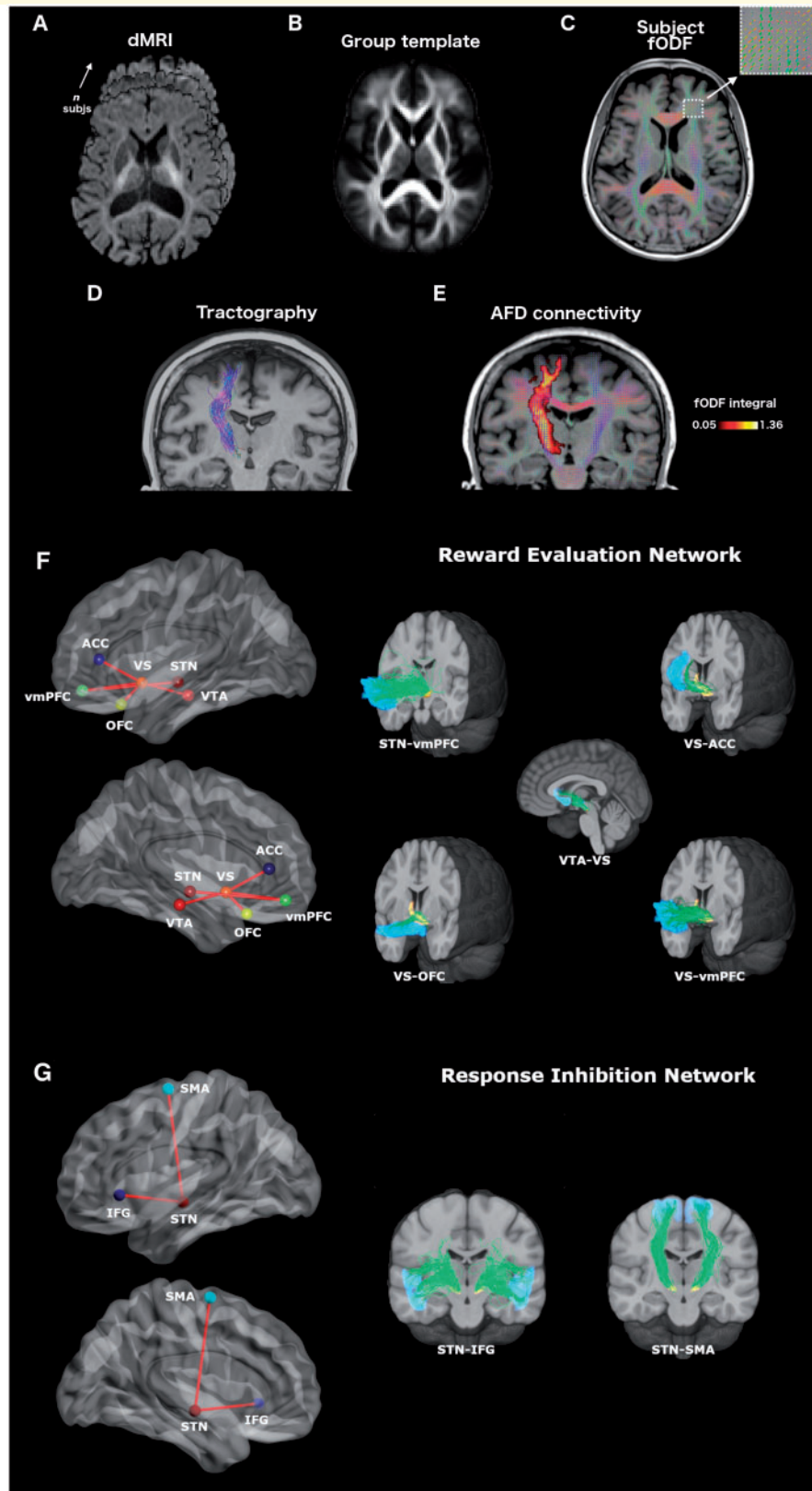


Figure 1 Diffusion processing pipeline. (A) High angular-resolution diffusion-weighted imaging was acquired along 90 directions using a 3 T scanner and a 64-channel array head coil, with a b -value of 3000s/mm^2 and voxel size of 1.7 mm^3 isotropic. After denoising, and correction for motion, susceptibility, bias and eddy-current induced distortions, fractional anisotropy (FA) maps were calculated for each participant. (B) FA maps were non-linearly registered to a population-average fractional anisotropy template, in order to derive an average white matter mask, which was then warped back into individual space to permit intensity normalization on the diffusion data. This ensured that the median b_0 white matter

ventral tegmental area (VTA). The connectivity of the STN with the vmPFC was also included in the reward evaluation network given the limbic connectivity of the STN (Haynes and Haber, 2013) and recent evidence suggesting changes in value sensitivity subsequent to STN-DBS for Parkinson's disease (Seymour *et al.*, 2016). The response inhibition network (Fig. 1G) included tracts connecting the STN with the IFG and the pre-SMA.

The cortical targets for these networks were selected from a gold-standard subdivision of the cortex based on multimodal MRI data (Glasser *et al.*, 2016), which were initially projected onto volumetric MNI ICBM non-linear asymmetric 2009a space (Horn, 2016). These included areas 10r and 10v (vmPFC), OFC and posterior OFC (OFC), a24 and p24 (ACC), 45 and 47l (IFG), 6ma and 6mp (SMA). The basal ganglia parcellations (within 2009b space), which served as seeds within these tractography networks, included the VS (Choi *et al.*, 2012), the VTA (Pauli *et al.*, 2018), and the STN (Ewert *et al.*, 2018). For VTA–VS connections, the VTA was defined as the seed region. All cortical and basal ganglia parcels were non-linearly transformed into native diffusion space via the skull-stripped anatomical image.

Data analysis

Principal components analysis

Amongst the neuropsychiatric instruments, principal components analysis (PCA) was first conducted. The motivation for this was to identify latent constructs of impulsivity across the questionnaires and clinician-administered tasks used in this investigation. Components with eigenvalues ≥ 1 were retained. We did not include behaviours derived from the virtual casino in this dimension-reduction step on account of the qualitative difference in the collection of these data (i.e. derived from virtual gameplay) and therefore hypothesized to represent 'purer', more ecologically-valid metrics of an individual participant's impulsivity.

Path modelling

Partial least squares path modelling (PLS-PM) was used to represent the multivariate relationships between anatomical and behavioural measures (McIntosh and Lobaugh, 2004; Shaw *et al.*, 2016), controlling for relevant demographic and

disease-related factors. PLS-PM is a form of structural equation modelling in which complex associations between multivariate datasets can be estimated. Each model specifies the linear weighting of one set of variables that best covaries with a linear weighting of another. For example, in this investigation, anatomical variables were created from the reward evaluation and response inhibition networks as a weighted mixture of the connectivity of each tract within the network. Behavioural variables were formed from each neuropsychiatric instrument and each gambling output (although as these were assessed individually, the relationship between each behavioural variable and observed behaviour was monotonic). Each model then represented the path coefficients and corresponding significance values for the relationship between these anatomical and behavioural variables; in addition to describing the weighted contribution that each tract made to the anatomical variable. In each model, continuous measures including age, years since diagnosis of Parkinson's disease and LEDD were also entered as covariates, with disease subtype and gender examined with a permutation test (Fig. 2). Interaction (or moderating) effects of these covariates on the effect of connectivity on behaviour were also modelled. Confidence intervals for 'out of sample' effects were determined by bootstrapping, in which the dataset was repeatedly sampled with replacement to create 10 000 independent bootstrapped datasets, with the sample size equal to the number of participants. Each PLS path model was developed using a bi-hemispheric anatomical network, but results for each hemisphere in isolation are also reported.

For each outcome of interest, a number of alternative PLS path models of varying complexity could be proposed, with no consensus method for determining the optimal trade-off between model fit and model complexity (Henseler and Sarstedt, 2013). Therefore, model complexity was constrained *a priori*; each PLS path model included only one anatomical network and all included age, years since diagnosis and LEDD as covariates. One interaction term with the anatomical network was included (e.g. the interaction of LEDD or age with the reward evaluation network). The winning model from all permutations was selected based on the maximum R^2 value prior to bootstrapping; in the setting of equivalent complexity of all estimated models, we thus use model fit (R^2) as the single summary metric for comparing models. To demonstrate that

Figure 1 Continued

value was uniform across the study population. (C) From the intensity-normalized diffusion data, signal responses across different tissue types (grey-matter, white-matter, CSF) were estimated and averaged across all participants to obtain a group-wise response function. Constrained spherical deconvolution of the average white-matter signal furnished fibre orientation distribution functions (fODF) for each participant. These functions provide local estimates of the density of fibres according to their angular orientation and can resolve complex organizations of crossing fibres more effectively than single tensor models. Our acquisition protocol incorporating 90 directions was designed to optimize this process. (D) Fibre bundles were reconstructed using a probabilistic streamline algorithm, through sampling a probability density of the fODF at each path point, tracking the most plausible fibre propagations between seed and target regions. (E) Quantitative estimates of structural connectivity between seed and target regions were derived from the apparent fibre density (AFD), calculated by summing the fODF lobe integrals along the pathway of interest and dividing by mean streamline length, to estimate the mean cross-sectional area of the fibre bundle. (F and G) Two discrete networks subserving reward evaluation and response inhibition were defined based on previous work. *Left*: Network models for each network. *Right*: Illustrative streamlines (green) from one participant connecting seed (orange) and target (blue) regions for each tract in the network. (F) The reward evaluation network included white matter tracts connecting the VS with the vmPFC, the OFC, the ACC and the VTA. It also included a tract connecting the STN with the vmPFC (the limbic hyperdirect pathway). (G) The response inhibition network included tracts connecting the STN with the IFG and the pre-SMA. *Left*: Network models for each network. Network models were visualized with the BrainNet Viewer (Xia *et al.*, 2013).

there were convincing dissociations by network (reward evaluation versus response inhibition) in the explanation of variance, results from the best performing model using the alternative network were also reported for each outcome variable. For example, a winning model that included the reward evaluation network was compared with models employing the response inhibition network, in order to quantify the difference in variance explained by the two alternative networks.

Impulse control behaviour status

In contrast to the QUIP-RS, which provides a dimensional rating of compulsive traits, we also applied a semi-structured clinical interview to delineate ICB status in a categorical manner. This interview took place with the participant and spousal caregiver and was completed by an experienced neuropsychiatrist (P.M.). An ICB was defined by the clinical diagnosis of pathological gambling, binge eating, compulsive shopping, hypersexuality, hobbyism or dopamine dysregulation in the presence of clinically-significant impairment or distress. ICB status was then examined with a permutation test in the PLS-PM approach, performed upon the winning model for each behavioural variable of interest. To evaluate the performance of models that differentiated participants by their ICB status, a repeated k -fold cross-validation was performed to evaluate the null hypothesis of no difference in model performance. Further details are provided in the Supplementary material.

Data analysis was performed in the R software environment (R Core Team, 2014), using the packages *FactoMineR* for PCA (Lê *et al.*, 2008), *pls* for PLS-PM (Sanchez, 2013), *pls* for PLS regression (Mevik and Wehrens, 2007) and *caret* for cross-validation (Kuhn, 2008).

Data availability

The gambling paradigm is provided for download on a git repository at https://github.com/saepaliwal/breakspear_slot_machine and the analysis pipeline at https://github.com/saepaliwal/dbs_pd_analysis_pipeline. The diffusion MRI processing pipeline is at <https://github.com/breakspear/diffusion-pipeline>. A de-identified dataset containing neuropsychiatric assessment and gambling data can be provided by P.E.M. (Philip.Mosley@qimrberghofer.edu.au) on application, subject to institutional review board approval.

Results

Participants

Sixty-three surgical candidates were consented. Three were unable to obtain diffusion MRI because of implanted prostheses incompatible with diffusion sequences, while one

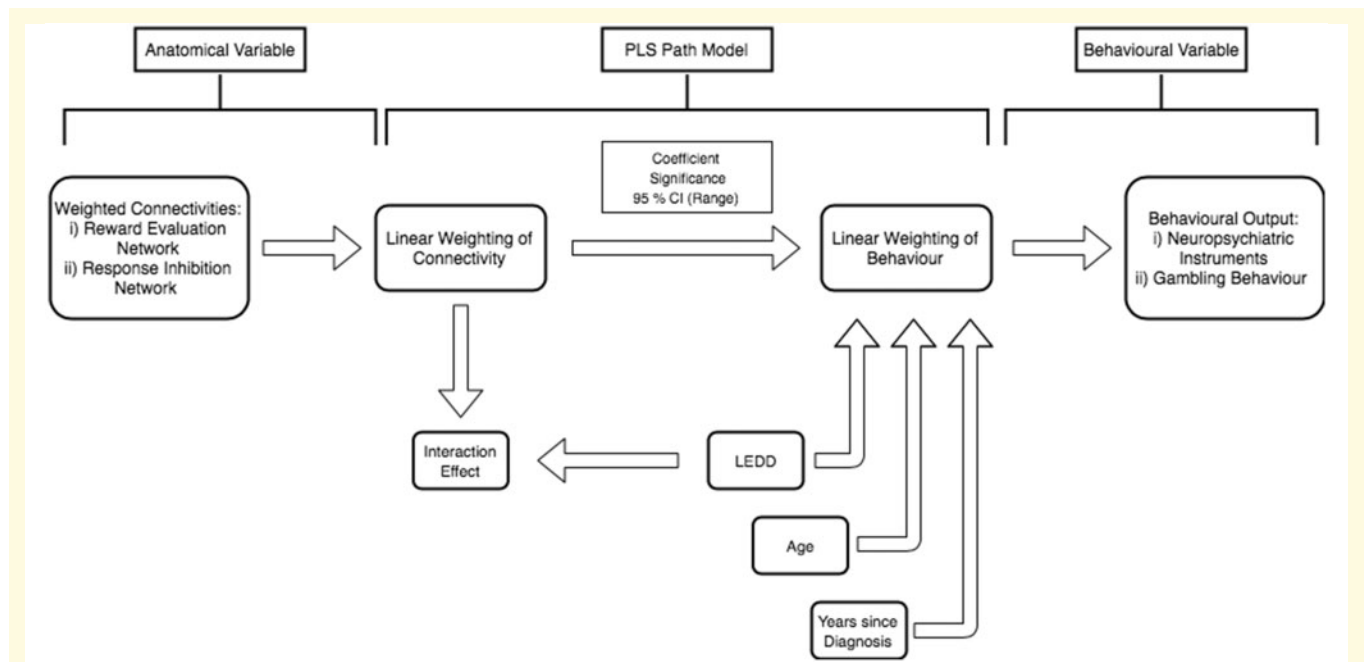


Figure 2 Partial least squares path modelling. A PLS path model represents the relationship between structural network connectivity and impulsivity. An anatomical variable is constructed from the connectivity of each white matter tract in the anatomical network under investigation. The individual contribution of each tract to the anatomical variable is quantified by a ‘weight’ and the anatomical variable is formed as a linear mixture of the corresponding connectivity values that best co-varies with the behavioural variable under investigation. The relationship between the anatomical and behavioural latent variables is quantified in the path model by a path coefficient (that can be tested for statistical significance). Relevant demographic and disease-related covariates are also represented and path coefficients can be determined for these relationships. An interaction (moderating) effect can be modelled; in this case, the interaction of LEDD with the anatomical variable. Bootstrapping of the model yields 95% confidence intervals (CI) for the path coefficients of interest.

was excluded because of excessive motion artefact in the diffusion images (manifesting as signal dropout in connected slices). One candidate was excluded because of extensive cerebrovascular disease (Fazekas grade IV), and another was excluded after being unable to complete the virtual casino prior to surgery because of fatigue. Thus, 57 participants proceeded to analysis (Table 1). Few participants ($n = 7$) engaged in the ‘cashout’ option within the virtual casino and this measure was therefore excluded from further analyses.

Seventeen participants had a current or past history of an ICB and six participants had more than one ICB, when these were evaluated as part of a clinical interview. These comprised pathological gambling ($n = 10$), hypersexuality ($n = 9$), compulsive shopping ($n = 3$), dopamine dysregulation ($n = 2$), binge eating ($n = 1$) and hobbyism ($n = 1$). ICB+ individuals had significantly higher scores on the QUIP-RS ($t = -4.31$, corrected $P = 0.003$) but there were no other significant differences in disease-related, neuropsychiatric or gambling measures by ICB status (Table 1).

Principal components analysis

PCA of the neuropsychiatric instruments revealed four dimensions (components) of impulsivity with eigenvalues of ≥ 1 , accounting for 77% of the total variance in the data (Table 2 and Supplementary Fig. 2). Dimension 1 was composed of equal contributions from the three subscales of the BIS and the QUIP-RS score, reflecting trait impulsiveness and compulsivity, and questionnaire-derived rather than task-related data. Dimension 2 reflected disinhibition, composed primarily from ELF Rule Violations. Dimension 3 reflected impatience, being made up of the Delay Discounting constant k . Finally, Dimension 4 again reflected disinhibition, composed primarily from the Hayling AB error score. The broad alignment of these dimensions with separate neuropsychiatric instruments suggested that there was little redundancy in the multimodal assessment of impulsivity in this investigation, aside from a distinction between questionnaire-based and examiner-administered measures. Given the equal contributions of the BIS subscales to Dimension 1 of the PCA, BIS total score was entered into the PLS path models.

Path modelling of connectivity and neuropsychiatric instruments

Path models using the neuropsychiatric instruments are presented first, followed by behavioural read-outs from the gambling paradigm. The neuropsychiatric instruments are presented in the order in which they appeared amongst orthogonal dimensions of the PCA, with questionnaire measures first, followed by examiner-administered tasks. The network (reward evaluation or response inhibition) explaining the maximum variance differed by variable according to the construct under examination. For the gambling outputs, the variance explained by path models

incorporating network indices was generally as high as or higher than for the neuropsychiatric variables (Table 3). For most measures, distinctions by hemisphere were observed and a distinction by ICB status was observed for the gambling variable ‘bet size’.

Barratt Impulsiveness Scale

We first assessed how variation in self-reported impulsiveness was related to the structural connectivity of our brain networks. The connectivity of the reward evaluation network and its interaction with LEDD best explained variations in this domain. The greater the connectivity of this network, the lower the self-reported impulsiveness (coefficient -0.44 , $P = 0.0021$; Table 3). The tracts weighted most strongly in the reward evaluation network were right VS-ACC and right STN-vmPFC (Fig. 3A and Supplementary Table 1). The connectivity of the reward evaluation network explained 12.8% of the total variance in BIS total score. The right ($P = 0.0028$) hemisphere in isolation evidenced a significant effect. There was no significant difference by ICB status on the effect of connectivity ($P = 0.41$).

Questionnaire for Impulsive-Compulsive disorders in PD Rating Scale

Last amongst the questionnaire measures, the connectivity of the reward evaluation network and its interaction with LEDD best explained variation in dimensional ratings of behavioural addictions such as gambling, sex, shopping and eating. The greater the connectivity of this network, the higher the rating of compulsivity (coefficient 0.34 , $P = 0.0045$, Table 3). The tracts weighted most strongly in the reward evaluation network were right VS-OFC, left VS-vmPFC and left VTA-VS (Fig. 3B and Supplementary Table 2). The effect of age (coefficient -0.30 , $P = 0.033$, younger age associated with greater compulsivity) and LEDD (coefficient 0.34 , $P = 0.040$, higher dose of dopaminergic medication associated with greater compulsivity) were also significant. The connectivity of the reward evaluation network explained 22.4% of the total variance in QUIP-RS score. The right ($P = 0.037$) hemisphere in isolation evidenced a significant effect. There was no significant difference by ICB status ($P = 0.84$) in the effect of connectivity.

Excluded Letter Fluency task rule violations

First amongst the examiner-administered tasks, we assessed how variation in disinhibition (as expressed by ELF rule violations) was related to the structural connectivity of our brain networks. The connectivity of the reward evaluation network and its interaction with age best explained variation in this facet of impulsivity. The greater the connectivity of

Table 1 Demographic and clinical characteristics of the Parkinson's disease cohort

Categorical variables	Total (n = 57)	
Gender, n (% total)		
Male	38 (66.6)	
Female	19 (33.3)	
Clinical subtype, n (% total)		
Akinetic-rigid	19 (33.3)	
Mixed	27 (47.4)	
Tremor	11 (19.3)	
ICB status, n (% total)		
Yes	17 (29.8)	
No	40 (70.2)	
Continuous variables, mean (SD), median [range]		ICB+ versus ICB-*
Age, years	62.2 (±9.7), 65 [35–77]	t = 2.84, corr. P = 0.059
Hoehn and Yahr stage	2.6 (±0.5), 2.5 [1.5–4]	t = -1.56, corr. P = 0.22
Years since diagnosis	8.2 (±4.1), 7 [2–21]	t = -0.80, corr. P = 0.52
LEDD	1124 (±618.6), 1025 [0–3450]	t = -1.89, corr. P = 0.21
BIS attentional	16.0 (±3.4), 16 [10–26]	t = -1.73, corr. P = 0.22
BIS non-planning	22.6 (±4.1), 23 [14–32]	t = -0.54, corr. P = 0.64
BIS motor	21.5 (±3.6), 21 [14–30]	t = -1.64, corr. P = 0.22
QUIP-RS total	19.4 (±15.4), 17 [0–63]	t = -4.31, corr. P = 0.003**
Delay Discount <i>k</i>	0.037 (±0.063), 0.016 [0.00016–0.25]	t = 2.42, corr. P = 0.076
Hayling AB Error Score	13.8 (±13.1), 9 [0–44]	t = 1.00, corr. P = 0.43
ELF rule violations	8.4 (±5.5), 8 [0–24]	t = -0.47, corr. P = 0.64
UPDRS Part III Motor	39.6 (±15.2), 39 [10–70]	t = 1.34, corr. P = 0.29
Virtual Casino, mean (SD), median [range]		
Average bet size, AUD	41.8 (±44.6), 27.2 [5–191.8]	t = 0.39, corr. P = 0.88
Machine switch, %	1.5 (±2.7), 0 [0–12]	t = 1.09, corr. P = 0.70
Double or nothing gamble, %	17.0 (±20.5), 15 [0–100]	t = 2.05, corr. P = 0.23

*FDR-corrected with Benjamini and Hochberg method (1995), with $\alpha = 0.05$.

Significance: ** $P < 0.01$, * $P < 0.05$.

UPDRS = Unified Parkinson's Disease Rating Scale.

Table 2 PCA of neuropsychiatric instruments

Measure	Representation	Dimension 1 Eigenvalue = 2.10	Dimension 2 Eigenvalue = 1.28	Dimension 3 Eigenvalue = 1.04	Dimension 4 Eigenvalue = 1.00
BIS attentional	Contribution	30.7%	-	-	-
	Correlation	0.80	-	-	-
BIS non-planning	Contribution	25.7%	-	-	-
	Correlation	0.74	-	-	-
BIS motor	Contribution	23.9%	-	-	-
	Correlation	0.71	-	-	-
QUIP-RS	Contribution	19.4%	-	-	-
	Correlation	0.64	-	-	-
Delay discount <i>k</i>	Contribution	-	-	60.7%	28.6%
	Correlation	-	-	0.79	-0.53
Hayling AB error score	Contribution	-	22.5%	-	56.8%
	Correlation	-	0.54	-	0.75
ELF rule violations	Contribution	-	55.6%	-	-
	Correlation	-	-0.84	-	-

this network, the fewer inhibitory errors (coefficient -0.58 , $P = 1.5 \times 10^{-5}$; Table 3). The tracts weighted most strongly in the reward evaluation network were right VS-vmPFC, right VTA-VS, right STN-vmPFC and left VS-ACC (Fig. 3C and Supplementary Table 3). The connectivity of the reward

evaluation network explained 32.7% of the total variance in ELF rule violations. The right ($P = 1.4 \times 10^{-4}$) hemisphere in isolation evidenced a significant effect. There was no significant difference by ICB status ($P = 0.14$) in the effect of connectivity.

Table 3 Detailed output of winning models from PLS-PM analysis

Model	Network	Interaction	R ²	Path coefficient	Significance, P	95% CI	Other significant covariates
Components of impulsivity							
BIS	Reward evaluation	Reward evaluation × LEDD	0.18	−0.44	0.0021**	−0.65 to −0.24	Nil
QUIP-RS	Reward evaluation	Reward evaluation × LEDD	0.37	0.34	0.0045**	0.065 to 0.57	(i) Age; <i>coeff</i> = −0.30; 95% CI = −0.52 to −0.058; <i>P</i> = 0.014 (ii) LEDD; <i>coeff</i> = 0.35; 95% CI = 0.12 to 1.10; <i>P</i> = 0.040
ELF rule violations	Reward evaluation	Reward evaluation × age	0.31	−0.58	1.5×10^{-5} ***	−0.78 to −0.31	Nil
Delay discount <i>k</i>	Reward evaluation	Reward evaluation × age	0.21	−0.49	8.0×10^{-4} ***	−0.75 to −0.19	Nil
Hayling AB error score	Response inhibition	Response inhibition × years since diagnosis	0.37	−0.54	8.0×10^{-5} ***	−0.72 to −0.34	Nil
Gambling behaviours							
Bet size	Reward evaluation	Reward evaluation × LEDD	0.34	0.42	0.0038**	0.15 to 0.65	Nil
Slot machine switch	Response inhibition	Response inhibition × years since diagnosis	0.30	−0.38	0.0027**	−0.60 to −0.15	(i) Interaction; <i>coeff</i> = 0.29; 95% CI = 0.075 to 0.50; <i>P</i> = 0.029
Double or nothing gambles	Reward evaluation	Reward evaluation × age	0.33	−0.41	0.0056**	−0.68 to −0.055	Nil

Significance: ****P* < 0.001, ***P* < 0.01.

Delay Discount *k*

We then looked at delay discounting: the tendency to prefer sooner, smaller rewards over those that are larger but temporally more distant. This was best explained by the connectivity of the reward evaluation network and its interaction with age. The greater the connectivity of this network, the lower the impatience and the higher the ability to defer reward (coefficient −0.49, *P* = 8.0×10^{-4} ; Table 3). The tracts weighted most strongly in the reward evaluation network were right VS-vmPFC, right VS-OFC and left VTA-VS (Fig. 3D and Supplementary Table 4). The connectivity of the reward evaluation network explained 18.2% of the total variance in the delay discount constant *k*. The right (*P* = 0.037) and left (*P* = 0.030) hemispheres in isolation evidenced a significant effect. There was no significant difference by ICB status (*P* = 0.24) in the effect of connectivity.

Hayling AB error score

Finally, the connectivity of the response inhibition network and its interaction with years since diagnosis of Parkinson's disease best explained variation in disinhibition (as expressed by Hayling A or B errors). The greater the connectivity of this network, the fewer inhibitory errors (coefficient −0.54, *P* = 1.7×10^{-5} ; Table 3). The tract weighted most strongly in the response inhibition network was left STN-SMA (Fig. 3E and Supplementary Table 5). The connectivity of the response inhibition network explained 26.2% of the total variance in

Hayling AB Error Score. The right (*P* = 0.0095) and left (*P* = 1.7×10^{-4}) hemispheres in isolation evidenced a significant effect. There was no significant difference by ICB status (*P* = 0.11) in the effect of connectivity.

Path modelling of connectivity and gambling behaviours

Bet size

A gambler's variation in bet size was best explained by the connectivity of the reward evaluation network and its interaction with LEDD. The greater the connectivity of the reward evaluation network, the greater the impulsivity as measured by risk taking, expressed as higher bets in the casino (coefficient 0.42, *P* = 0.0038; Table 3). The most heavily weighted tracts in the reward evaluation network were right VS-vmPFC and left VS-vmPFC (Fig. 4A and Supplementary Table 6). The connectivity of the reward evaluation network explained 29.7% of the total variance in bet size. Both the right (*P* = 0.017) and left hemispheres (*P* = 0.0021) in isolation evidenced a significant effect. Notably, there was a significant difference by ICB status on the effect of connectivity (coefficient ICB+ = −0.87, coefficient ICB− = 0.45, *P* = 0.0099). There was also a significant difference by ICB status in the interaction of LEDD with connectivity (coefficient ICB+ = −0.39, coefficient ICB− = 1.53, *P* = 0.030).

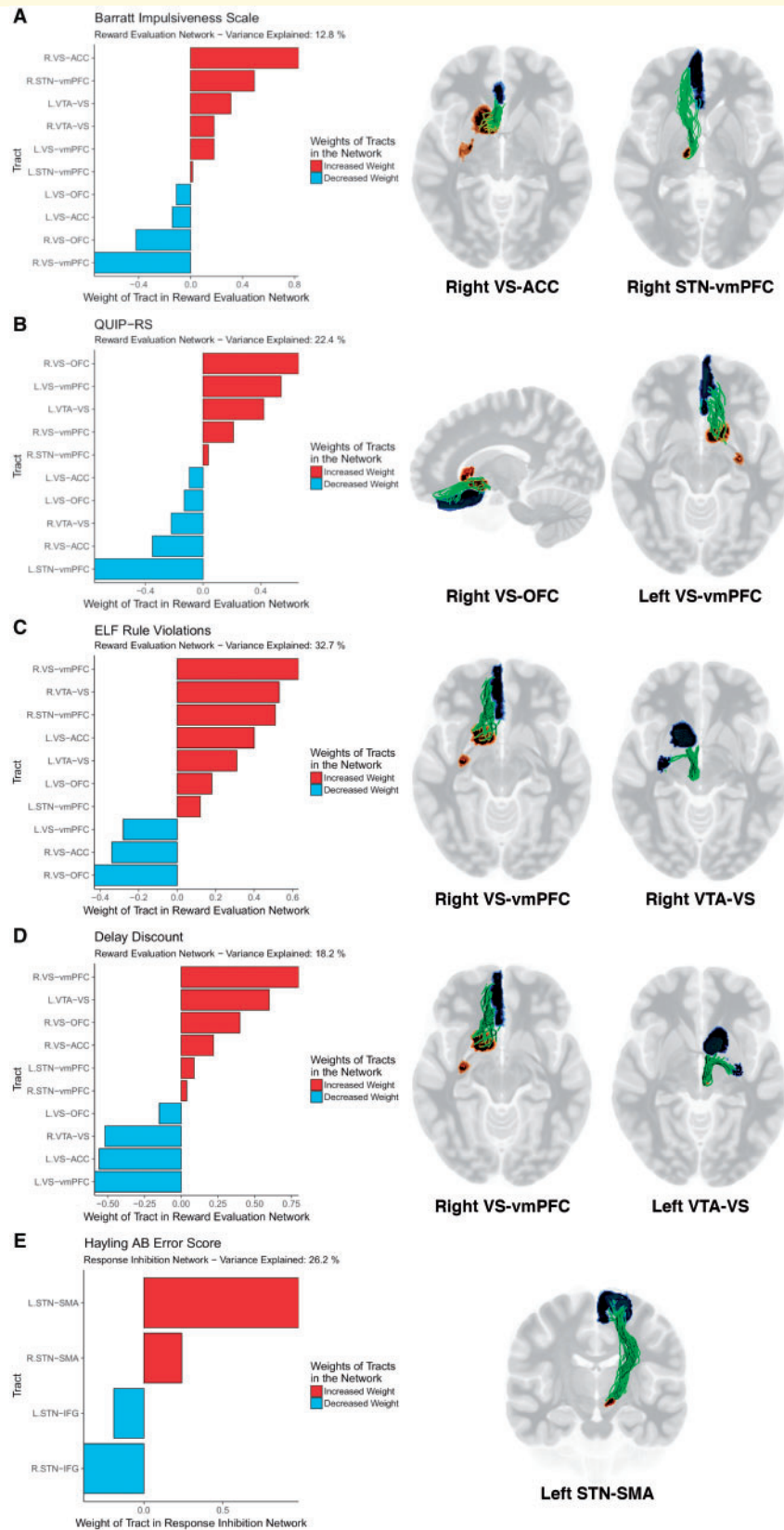


Figure 3 Network influences on impulsivity. The association of structural connectivity with components of impulsivity derived from neuropsychiatric instruments. *Left:* Bar plot displaying the relative weights of each tract in the winning network. Blue = negative weight, red = positive weight. *Right:* Illustrative streamlines (green) from an exemplar participant connecting seed (orange) and target (blue) regions for each heavily weighted tract in the network. L = left hemisphere; R = right hemisphere.

Slot machine switch

A gambler's tendency to switch between slot machines in the virtual casino was best explained by the connectivity of the response inhibition network and its interaction with years since diagnosis of Parkinson's disease. The greater the connectivity of the response inhibition network, the more likely a gambler was to prioritize exploitation over exploration (i.e. less likely to switch machines) (coefficient -0.38 , $P = 0.0027$; Table 3). The interaction effect of years since diagnosis with connectivity was also significant (coefficient 0.29 , $P = 0.029$). The most heavily weighted tracts in the response inhibition network were right STN-SMA and right STN-IFG (Fig. 4B and Supplementary Table 7). The connectivity of the response inhibition network explained 21.7% of the total variance in slot machine switch. Neither hemisphere in isolation evidenced a significant effect. There was no significant difference by ICB status on the effect of connectivity ($P = 0.47$).

Double or nothing gambles

A gambler's tendency to accept double or nothing gambles was best explained by the connectivity of the reward evaluation network and its interaction with age. In contrast with bet size, the greater the connectivity of the reward evaluation network, the less explorative the gambler, with a lower likelihood of accepting a double or nothing gamble (coefficient -0.41 , $P = 0.0056$; Table 3). Again, in contrast with bet size, the most heavily weighted tracts in the reward evaluation network were the left VS-OFC and left STN-vmPFC, whilst the bilateral VS-vmPFC tract weighted negatively (Fig. 4C and Supplementary Table 8). The connectivity of the reward evaluation network explained 24.1% of the total variance in double or nothing gamble uptake. The left ($P = 0.027$) hemisphere in isolation evidenced a significant effect. There was no significant difference by ICB status on the effect of connectivity ($P = 0.14$).

Cross validation of bet size by ICD status

The finding that ICB+ individuals could be distinguished by the effect of connectivity on gambling behaviour (bet size) was evaluated with repeated k -fold cross-validation. This model yielded a receiver operating curve (ROC) area under the curve (AUC) of 0.72, a sensitivity of 0.89 and a specificity of 0.38. When compared with a null (chance) model there was a significant difference in ROC AUC (model = 0.72, null = 0.64 $P = 2.2 \times 10^{-15}$) (Fig. 5). There was also a significant difference in specificity (model = 0.38, null = 0.094 $P = 2.2 \times 10^{-16}$).

Supplementary analyses

To evaluate the specificity of each network (response inhibition or reward evaluation) in explaining the variance of each construct under examination, findings for the best model from the alternative network are presented in Supplementary Table 9. Again, this was defined as the model with the maximum R^2 , allowing LEDD, age and years since diagnosis of Parkinson's disease as an

interaction effect with network connectivity. Findings demonstrated that the winning network model explained considerably more variance than the 'second placed' model using the alternative network. Furthermore, for the majority of constructs, the effect of connectivity for the alternative network did not reach statistical significance or the bootstrapped 95% confidence intervals cross zero.

Discussion

We found that the structural connectivity of cortico-subcortical networks contributes significantly to variability in impulsivity and gambling behaviours amongst individuals with Parkinson's disease prior to subthalamic DBS. The variance explained by connectivity was highest for behavioural indices of impulsivity, derived from clinic-based tasks and a naturalistic virtual casino. The contribution of each network and the relative influence of each hemisphere were dissociated by the neuropsychiatric construct or gambling behaviour under investigation, supporting the conceptualization of impulsivity as a multifaceted construct. Furthermore, individuals with a history of ICBs could be differentiated from those without ICBs in the virtual casino when the interaction of betting behaviour, dopaminergic dosage and structural connectivity was examined.

Amongst the neuropsychiatric instruments, we identified distinct dimensions (components) of impulsivity based upon a comprehensive phenotyping of participants. Broadly, these orthogonal dimensions derived from the PCA mapped onto distinct neuropsychiatric instruments, suggesting that our battery assessed different facets of impulsivity in this cohort. However, it is also notable that the first dimension of the PCA was composed of metrics derived from self-rated questionnaires, raising the possibility that this dimension represented response modality rather than impulsivity *per se*. This is interesting in the light of a recent comparable finding amongst individuals with frontotemporal dementia, in which questionnaire measures separated from experimental tasks in the characterization of impulsivity and apathy (Lansdall *et al.*, 2017).

When the neuropsychiatric instruments were examined individually, interindividual variability in the BIS, the QUIP-RS, the Delay Discounting task and ELF rule violations were best accounted for by PLS path models incorporating the reward evaluation network—a network composed of bilateral fibre tracts connecting the STN, VS, VTA, OFC, ACC and vmPFC. The most heavily weighted tracts within the reward evaluation network differed between each of these instruments. Moreover, the influence of connectivity differed in direction (positive or negative) amongst the different constructs. For instance, for QUIP-RS score, heavily weighted tracts involved the VS, VTA, OFC and vmPFC, with greater connectivity associated with greater impulsivity and a bias to the right hemisphere. However, for BIS score, ELF rule violations and Delay Discounting k , greater connectivity of the network

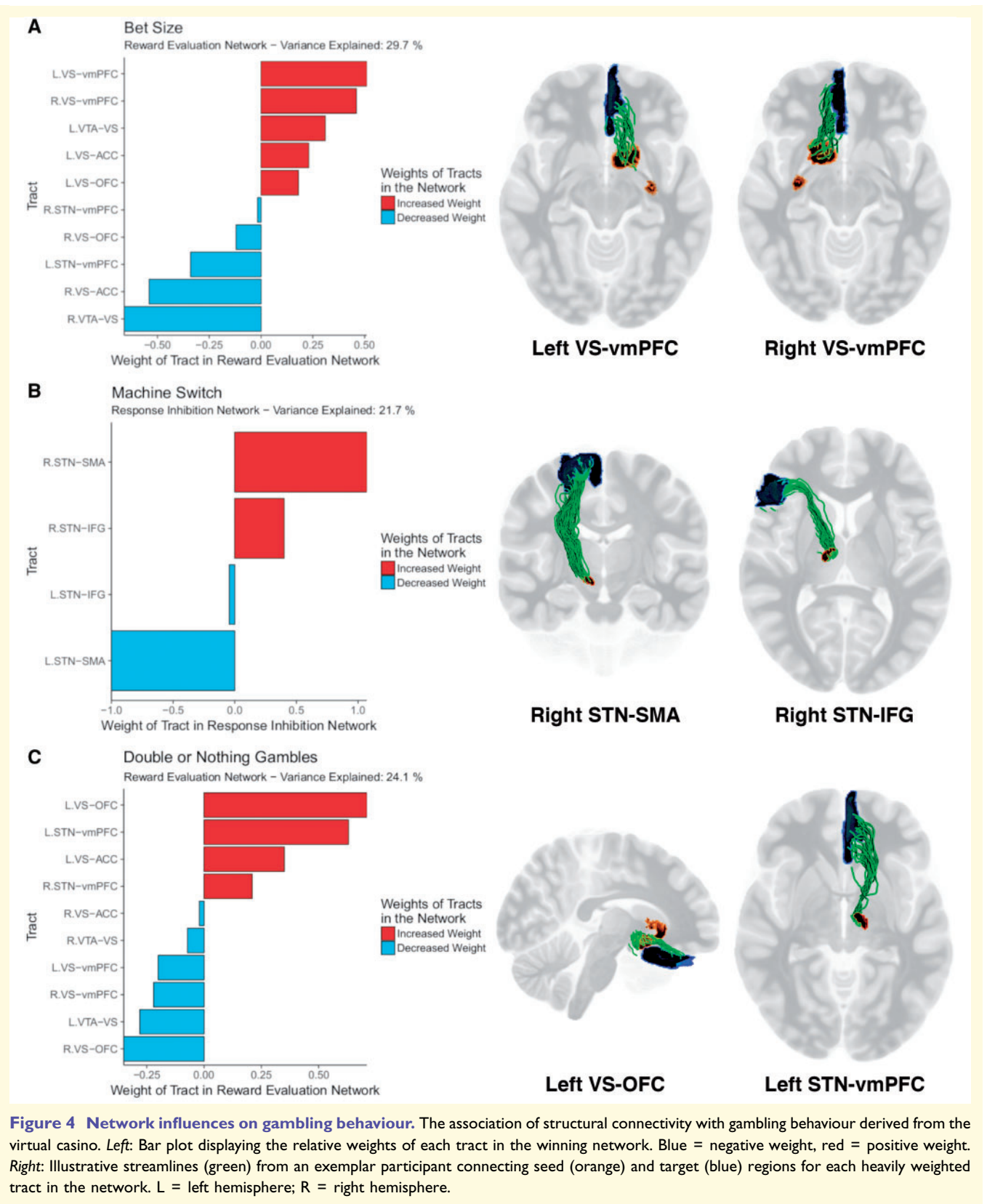


Figure 4 Network influences on gambling behaviour. The association of structural connectivity with gambling behaviour derived from the virtual casino. *Left:* Bar plot displaying the relative weights of each tract in the winning network. Blue = negative weight, red = positive weight. *Right:* Illustrative streamlines (green) from an exemplar participant connecting seed (orange) and target (blue) regions for each heavily weighted tract in the network. L = left hemisphere; R = right hemisphere.

was associated with reduced impulsivity. This dissociation may be attributable to differences in the construct assessed in each task (such as the difference between impatience and

compulsiveness), as well as to differences in the individual weightings of each tract within the reward evaluation network. For example, for BIS score and ELF rule violations,

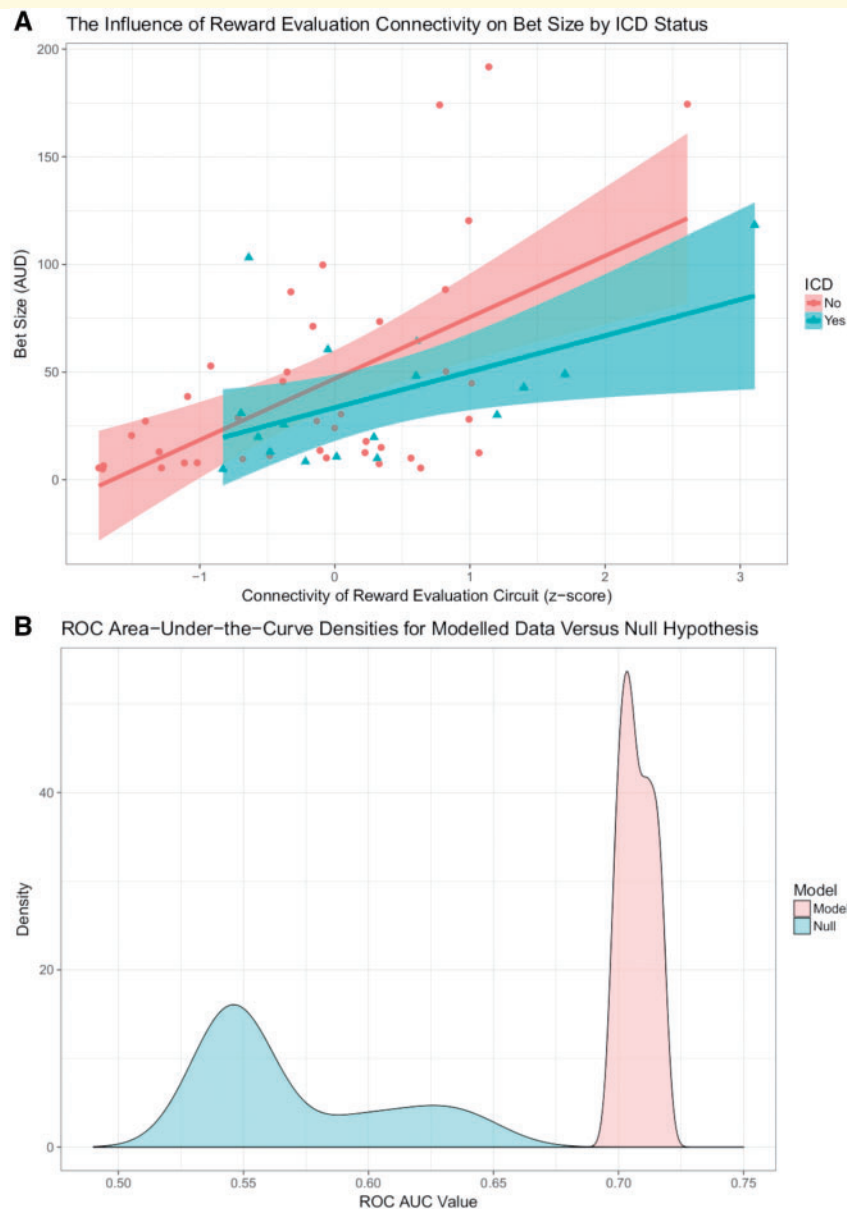


Figure 5 Cross-validation of the relationship between ICB status, connectivity and bet size. **(A)** The relationship between connectivity of the reward evaluation network and bet size in the virtual casino, plotted by ICB status. Shaded area = standard error. **(B)** Distribution of the receiver operating curve (ROC) area under the curve (AUC) values for a repeated *k*-fold cross validation model, comparing a null model (with a shuffled dependent variable) against a model trained on the relationship between connectivity and bet size.

heavily weighted tracts included those connecting the STN with the vm PFC, suggesting that the strength of the stopping signal exerted by the STN made a key contribution to the role of this network. These ‘hyperdirect’ tracts may be a means through which the STN links reward evaluation and response inhibition networks (Nambu *et al.*, 2002; Haynes and Haber, 2013). Again, right-hemispheric tracts were predominant in this measure of inhibitory control. This bias is interesting, given prior work suggesting that the executive control of inhibition is primarily a right-lateralized process (Aron *et al.*, 2004; Possin *et al.*, 2009; D’Alberty *et al.*, 2017) and that modulation of the right

STN after DBS for Parkinson’s disease is most likely to induce disinhibition (Mosley *et al.*, 2018b).

Amongst the neuropsychiatric instruments, only inter-individual variability in the Hayling AB Error score was best accounted for by a PLS path model incorporating the response inhibition network—a network composed of bilateral fibre tracts connecting the STN, SMA and IFG. The greater the connectivity of this network, the less impulsive were the participants according to this examiner-administered metric. The weighting of tracts in this model is consistent with the classic ‘stopping’ network (Aron *et al.*, 2007; Rae *et al.*, 2015) and accords with the nature of

the behaviours represented in this task, where participants must suppress habitual responding.

Although they both assess disinhibition, Hayling AB errors and ELF rule violations correlate in opposite directions on Dimension 2 and are influenced most strongly by different networks when examined independently. This parallels prior findings using voxel-based morphometry, which have implicated the IFG in Hayling inhibitory errors and the OFC and VS in ELF Rule Violations (O'Callaghan *et al.*, 2013a, b). This may be related to underlying differences in the fine-grained structure of each task. In the ELF task, participants must obey phonemic policies, whereas in the Hayling test, participants must monitor semantic rules and implement a strategy to avoid suppression errors. In addition, to produce rule violations in the ELF task, the participant must be sufficiently 'energized' to initiate and maintain the generation of words (phonemic verbal fluency), which presumably requires the integrity of dopaminergic networks such as those involving the VTA and VS (McAuley, 2003; Barker *et al.*, 2018). Furthermore, in the Hayling test, participants can make both gross failures of inhibition (A errors) or more subtle errors of semantics (B errors). In lesion studies, phonemic word fluency deficits are associated with the left IFG (Robinson *et al.*, 2012) and Hayling semantic errors with the right IFG (Robinson *et al.*, 2015). However, in the present cohort, the tract connecting the left STN-SMA was most strongly implicated in interindividual variability in the Hayling AB error score. Further work will clarify the contribution of these tracts to these aspects of response inhibition.

As highlighted above, the brain-behaviour covariations were as high or higher for gambling behaviours in the virtual casino as compared to the clinician-administered tasks. The greater the connectivity of the reward evaluation network, the more explorative and the higher the bet size used by participants, modulated by LEDD. Bilateral tracts connecting the VS to vmPFC were weighted most heavily in this model, upholding much prior work linking the VS with reinforcement learning and reward evaluation (Schultz *et al.*, 1997; Abler *et al.*, 2006; Daw *et al.*, 2006; Tanaka *et al.*, 2008; Wittmann *et al.*, 2008; Basar *et al.*, 2010; Haber and Knutson, 2010; de Wit *et al.*, 2012; Kishida *et al.*, 2016; Hampton *et al.*, 2017). The amount wagered in a gamble is a parsimonious way to obtain a behavioural readout of impulsivity and it is interesting that this measure correlated significantly with our reward evaluation network measures.

The tendency of gamblers to switch slot machines in the virtual casino was negatively correlated with the connectivity of the response inhibition network, modulated by years since diagnosis. Gamblers with reduced connectivity of the response inhibition network were more likely to be impatient and explore different slot machines and thus could be considered more impulsive on this measure, preferring to explore their current environment rather than exploit alternatives. Again, right hemispheric tracts were weighted most strongly within this network. Here, the

effect of years since diagnosis may be related to progressive neurodegeneration and the vulnerability of connections between the STN and SMA, given that modulation of these connections is most likely to result in a therapeutic benefit after STN-DBS for Parkinson's disease (Vanegas-Arroyave *et al.*, 2016).

Finally, the lesser the connectivity of the reward evaluation network, the more likely gamblers were to accept double or nothing gambles. This appears at first paradoxical when evaluated against the results for bet size. Specifically, when double or nothing gambles are considered, participants with greater connectivity of the reward evaluation network are less likely to take risks. However, when the weightings of the network are examined (Fig. 4 and Supplementary material), the distribution of weightings is quite different to the network evaluated for bet size. In the reward evaluation network for double or nothing gambles, the VS-vmPFC tracts are now negatively-weighted, with the most highly-weighted tract being the left VS-OFC. The tracts from STN to vmPFC are also upweighted (again, a means through which the STN links reward evaluation and response inhibition networks). Thus, the connectivity of the reward evaluation network may have dissociable effects on different aspects of impulsive behaviour, with associations in opposite directions depending upon the cognitive operation under study. This supports prior work demonstrating that greater frontostriatal connectivity is associated with the ability to delay gratification in young adults (Peper *et al.*, 2013; Achterberg *et al.*, 2016).

Crucially, our paradigm was able to identify significant differences between participants by ICB status. Individuals with a history of an ICB differed in the effect of reward evaluation connectivity on bet size, and the interaction effect of LEDD with reward evaluation connectivity. This finding is in line with previous work demonstrating that individuals with ICBs differ in their neural response to dopaminergic medication (van Eimeren *et al.*, 2010; Voon *et al.*, 2011) and that striatal dopaminergic transmission is altered in ICB+ individuals (Stark *et al.*, 2018). Our cross-validation results suggest this is not merely a chance effect, although we stress that we do not propose that our model (in its current form) could be used to differentiate prospectively between ICB+ and ICB- individuals, given its low specificity and the likelihood of a high false-positive rate. Nevertheless, using a game-like assay to obtain a behavioural (and, in the future, possibly also neural) signature of impulsivity is an appealing prospect. To our knowledge this report offers the first structural account of brain-behaviour covariation in Parkinson's disease.

Limitations of this investigation include the cross-sectional design, which precludes causal inferences about the link between structural connectivity and impulsivity. Furthermore, the pre-surgical nature of the sampled population means that these findings may not apply to all individuals with Parkinson's disease; there may be cohort-level differences in impulsivity amongst those who proceed to neurosurgery for their movement disorder.

A further limitation with the virtual casino task that we use is its exclusive basis in gambling behaviour. Seven of our 17 participants with clinically-significant ICBs did not express pathological gambling as a feature of their compulsive behaviours, whilst in the wider Parkinson's disease population, pathological gambling is certainly not seen in all individuals with ICBs. We endeavoured to mitigate this problem by including bright colours and noises in our virtual casino that would have a universally appetitive influence, but we cannot discount the possibility that there may be a more suitable 'domain general' behavioural paradigm that could be developed to encompass all individuals with varied ICBs.

In summary, significant dimensional variations in impulsivity and compulsive behaviours are seen amongst individuals with Parkinson's disease. However, it has been unclear if these relate to underlying differences in brain networks likely to be affected by neurodegeneration and dopaminergic therapies. Distinct reward evaluation and response inhibition networks may associate with dissociable aspects of impulsivity (*cf.* choosing and stopping) according to the behaviour under investigation. In our cohort, we have shown that impulsivity can be decomposed into non-overlapping components with separate neural covariations, grounded in these aforementioned brain networks. Importantly, clinician-administered tasks and ecologically valid measures derived from a naturalistic gambling were more closely tied to structural connectivity measures than traditional neuropsychiatric questionnaires. During the gambling task, participants with a history of ICBs differed from other individuals in the manner in which their connectivity strengths interacted with dopaminergic therapy and gambling behaviour. This raises the possibility of using similar methods in clinical settings, as a means to identify those at risk of harmful behaviour.

Acknowledgements

The authors gratefully acknowledge the commitment of participants and caregivers who contributed their time to this study. The authors acknowledge the ongoing support of St Andrew's War Memorial Hospital and the Herston Imaging Research Facility.

Funding

P.E.M. was supported by an early career fellowship from the Queensland government's 'Advance Queensland' initiative, a Royal Brisbane and Woman's Hospital Foundation Research Grant and a young investigator grant from the Royal Australian and New Zealand College of Psychiatrists. He received an unrestricted educational grant from Medtronic. M.B. was supported by the National Health and Medical Research Council (118153, 10371296, 1095227) and the Australian Research Council (CE140100007). K.E.S. was supported by the University of

Zurich and the René and Susanne Braginsky Foundation. A.P. acknowledges the current support of Dr Douglas Garrett's funding from the Emmy Noether Programme grant (German Research Council) and the Max Planck UCL Centre for Computational Psychiatry and Ageing Research.

Competing interests

All authors report no competing interests.

Supplementary material

Supplementary material is available at *Brain* online.

References

- Abler B, Walter H, Erk S, Kammerer H, Spitzer M. Prediction error as a linear function of reward probability is coded in human nucleus accumbens. *NeuroImage* 2006; 31: 790–5.
- Accolla EA, Herrojo Ruiz M, Horn A, Schneider GH, Schmitz-Hubsch T, Draganski B, et al. Brain networks modulated by subthalamic nucleus deep brain stimulation. *Brain* 2016; 139: 2503–15.
- Achterberg M, Peper JS, van Duijvenvoorde AC, Mandl RC, Crone EA. Frontostriatal white matter integrity predicts development of delay of gratification: a longitudinal study. *J Neurosci* 2016; 36: 1954–61.
- Akram H, Sotiropoulos SN, Jbabdi S, Georgiev D, Mählknecht P, Hyam J, et al. Subthalamic deep brain stimulation sweet spots and hyperdirect cortical connectivity in Parkinson's disease. *NeuroImage* 2017; 158: 332–45.
- Andersson JLR, Sotiropoulos SN. An integrated approach to correction for off-resonance effects and subject movement in diffusion MR imaging. *NeuroImage* 2016; 125: 1063–78.
- Antonelli F, Ko JH, Miyasaki J, Lang AE, Houle S, Valzania F, et al. Dopamine-agonists and impulsivity in Parkinson's disease: impulsive choices vs. impulsive actions. *Hum Brain Mapp* 2014; 35: 2499–506.
- Antonini A, Siri C, Santangelo G, Cilia R, Poletti M, Canesi M, et al. Impulsivity and compulsivity in drug-naive patients with Parkinson's disease. *Mov Disord* 2011; 26: 464–8.
- Aron AR. From reactive to proactive and selective control: developing a richer model for stopping inappropriate responses. *Biol Psychiatry* 2011; 69: e55–68.
- Aron AR, Behrens TE, Smith S, Frank MJ, Poldrack RA. Triangulating a cognitive control network using diffusion-weighted magnetic resonance imaging (MRI) and functional MRI. *J Neurosci* 2007; 27: 3743–52.
- Aron AR, Robbins TW, Poldrack RA. Inhibition and the right inferior frontal cortex. *Trends Cogn Sci* 2004; 8: 170–7.
- Barker MS, Nelson NL, O'Sullivan JD, Adam R, Robinson GA. Enlargement and spoken language production: evidence from progressive supranuclear palsy. *Neuropsychologia* 2018; 119: 349–62.
- Basar K, Sesia T, Groenewegen H, Steinbusch HW, Visser-Vandewalle V, Temel Y. Nucleus accumbens and impulsivity. *Prog Neurobiol* 2010; 92: 533–57.
- Burgess PW, Shallice T; Thames Valley Test Company. The Hayling and Brixton tests. Bury St Edmunds: Thames Valley Test Company; 1997.
- Carriere N, Lopes R, Defebvre L, Delmaire C, Dujardin K. Impaired corticostriatal connectivity in impulse control disorders in Parkinson disease. *Neurology* 2015; 84: 2116–23.

- Chen Y, Ge S, Li Y, Li N, Wang J, Wang X, et al. Role of the cortico-subthalamic hyperdirect pathway in deep brain stimulation for the treatment of Parkinson disease: a diffusion tensor imaging study. *World Neurosurg* 2018; 114: e1079–85.
- Choi EY, Yeo BT, Buckner RL. The organization of the human striatum estimated by intrinsic functional connectivity. *J Neurophysiol* 2012; 108: 2242–63.
- Cilia R, Cho SS, van Eimeren T, Marotta G, Siri C, Ko JH, et al. Pathological gambling in patients with Parkinson's disease is associated with fronto-striatal disconnection: a path modeling analysis. *Mov Disord* 2011; 26: 225–33.
- Claassen DO, van den Wildenberg WP, Ridderinkhof KR, Jessup CK, Harrison MB, Wooten GF, et al. The risky business of dopamine agonists in Parkinson disease and impulse control disorders. *Behav Neurosci* 2011; 125: 492–500.
- D'Albeto N, Funnell M, Potter A, Garavan H. A split-brain case study on the hemispheric lateralization of inhibitory control. *Neuropsychologia* 2017; 99: 24–9.
- Daw ND, O'Doherty JP, Dayan P, Seymour B, Dolan RJ. Cortical substrates for exploratory decisions in humans. *Nature* 2006; 441: 876–9.
- de Wit S, Watson P, Harsay HA, Cohen MX, van de Vijver I, Ridderinkhof KR. Corticostriatal connectivity underlies individual differences in the balance between habitual and goal-directed action control. *J Neurosci* 2012; 32: 12066–75.
- Djamshidian A, O'Sullivan SS, Foltynie T, Aviles-Olmos I, Limousin P, Noyce A, et al. Dopamine agonists rather than deep brain stimulation cause reflection impulsivity in Parkinson's disease. *J Parkinson's Dis* 2013; 3: 139–44.
- Djamshidian A, O'Sullivan SS, Sanotsky Y, Sharman S, Matviyenko Y, Foltynie T, et al. Decision making, impulsivity, and addictions: do Parkinson's disease patients jump to conclusions? *Mov Disord* 2012; 27: 1137–45.
- Emre M, Aarsland D, Brown R, Burn DJ, Duyckaerts C, Mizuno Y, et al. Clinical diagnostic criteria for dementia associated with Parkinson's disease. *Mov Disord* 2007; 22: 1689–707.
- Evans AH, Katzenschlager R, Paviour D, O'Sullivan JD, Appel S, Lawrence AD, et al. Punding in Parkinson's disease: its relation to the dopamine dysregulation syndrome. *Mov Disord* 2004; 19: 397–405.
- Ewert S, Pletting P, Li N, Chakravarty MM, Collins DL, Herrington TM, et al. Toward defining deep brain stimulation targets in MNI space: a subcortical atlas based on multimodal MRI, histology and structural connectivity. *NeuroImage* 2018; 170: 271–82.
- Frank MJ, Seeberger LC, O'Reilly RC. By carrot or by stick: cognitive reinforcement learning in Parkinsonism. *Science* 2004; 306: 1940–3.
- Gauggel S, Rieger M, Feghoff TA. Inhibition of ongoing responses in patients with Parkinson's disease. *J Neurol Neurosurg Psychiatry* 2004; 75: 539–44.
- Glasser MF, Coalson TS, Robinson EC, Hacker CD, Harwell J, Yacoub E, et al. A multi-modal parcellation of human cerebral cortex. *Nature* 2016; 536: 171–8.
- Goto Y, Grace AA. Dopaminergic modulation of limbic and cortical drive of nucleus accumbens in goal-directed behavior. *Nat Neurosci* 2005; 8: 805–12.
- Grace AA. Physiology of the normal and dopamine-depleted basal ganglia: insights into levodopa pharmacotherapy. *Mov Disord* 2008; 23: S560–9.
- Haber SN, Knutson B. The reward circuit: linking primate anatomy and human imaging. *Neuropsychopharmacology* 2010; 35: 4–26.
- Hampton WH, Alm KH, Venkatraman V, Nugiel T, Olson IR. Dissociable frontostriatal white matter connectivity underlies reward and motor impulsivity. *NeuroImage* 2017; 150: 336–43.
- Haynes WI, Haber SN. The organization of prefrontal-subthalamic inputs in primates provides an anatomical substrate for both functional specificity and integration: implications for Basal Ganglia models and deep brain stimulation. *J Neurosci* 2013; 33: 4804–14.
- Henseler J, Sarstedt M. Goodness-of-fit indices for partial least squares path modeling. *Comput Stat* 2013; 28: 565–80.
- Hoehn MM, Yahr MD. Parkinsonism: onset, progression and mortality. *Neurology* 1967; 17: 427–42.
- Horn A. HCP-MMP1.0 Projected on MNI2009a GM (Volumetric) in NIfTI Format. 2016. <https://neurovault.org/images/24150/> (3 August 2018, date last accessed).
- Horn A, Reich M, Vorwerk J, Li N, Wenzel G, Fang Q, et al. Connectivity predicts deep brain stimulation outcome in Parkinson disease. *Ann Neurol* 2017; 82: 67–78.
- Hughes AJ, Daniel SE, Kilford L, Lees AJ. Accuracy of clinical diagnosis of idiopathic Parkinson's disease: a clinico-pathological study of 100 cases. *J Neurol Neurosurg Psychiatry* 1992; 55: 181–4.
- Imperiale F, Agosta F, Canu E, Markovic V, Inuggi A, Jecmenica-Lukic M, et al. Brain structural and functional signatures of impulsive-compulsive behaviours in Parkinson's disease. *Mol Psychiatry* 2018; 23: 459–66.
- Jbabdi S, Sotiropoulos SN, Haber SN, Van Essen DC, Behrens TE. Measuring macroscopic brain connections in vivo. *Nat Neurosci* 2015; 18: 1546–55.
- Jeurissen B, Tournier JD, Dhollander T, Connelly A, Sijbers J. Multi-tissue constrained spherical deconvolution for improved analysis of multi-shell diffusion MRI data. *NeuroImage* 2014; 103: 411–26.
- Johnson JG, Busemeyer JR. Decision making under risk and uncertainty. *Wiley Interdiscip Rev Cogn Sci* 2010; 1: 736–49.
- Kirby KN, Petry NM, Bickel WK. Heroin addicts have higher discount rates for delayed rewards than non-drug-using controls. *J Exp Psychol Gen* 1999; 128: 78–87.
- Kish SJ, Shannak K, Hornykiewicz O. Uneven pattern of dopamine loss in the striatum of patients with idiopathic Parkinson's disease. Pathophysiologic and clinical implications. *N Engl J Med* 1988; 318: 876–80.
- Kishida KT, Saez I, Lohrenz T, Witcher MR, Laxton AW, Tatter SB, et al. Subsecond dopamine fluctuations in human striatum encode superposed error signals about actual and counterfactual reward. *Proc Natl Acad Sci U S A* 2016; 113: 200–5.
- Knutson B, Fong GW, Adams CM, Varner JL, Hommer D. Dissociation of reward anticipation and outcome with event-related fMRI. *Neuroreport* 2001; 12: 3683–7.
- Kobayakawa M, Koyama S, Mimura M, Kawamura M. Decision making in Parkinson's disease: Analysis of behavioral and physiological patterns in the Iowa gambling task. *Mov Disord* 2008; 23: 547–52.
- Kolling N, Behrens T, Wittmann MK, Rushworth M. Multiple signals in anterior cingulate cortex. *Curr Opin Neurobiol* 2016; 37: 36–43.
- Kuhn M. Building predictive models in R using the caret package. *J Stat Softw* 2008; 28(5): 1–26.
- Kumakura Y, Danielsen EH, Gjedde A, Vernaleken I, Buchholz H-G, Heintz A, et al. Elevated [18F] FDOPA utilization in the periaqueductal gray and medial nucleus accumbens of patients with early Parkinson's disease. *NeuroImage* 2010; 49: 2933–9.
- Lansdall CJ, Coyle-Gilchrist ITS, Jones PS, Vazquez Rodriguez P, Wilcox A, Wehmann E, et al. Apathy and impulsivity in frontotemporal lobar degeneration syndromes. *Brain* 2017; 140: 1792–807.
- Lê S, Josse J, Hussen F. FactoMineR: An R package for multivariate analysis. *J Stat Softw* 2008; 25: 1–18.
- McAuley JH. The physiological basis of clinical deficits in Parkinson's disease. *Prog Neurobiol* 2003; 69: 27–48.
- McIntosh AR, Lobaugh NJ. Partial least squares analysis of neuroimaging data: applications and advances. *NeuroImage* 2004; 23: S250–63.
- Mevik B-H, Wehrens R. The pls package: principal component and partial least squares regression in R. *J Stat Softw* 2007; 18: 1–23.
- Milenkova M, Mohammadi B, Kollewe K, Schrader C, Fellbrich A, Wittfoth M, et al. Intertemporal choice in Parkinson's disease. *Mov Disord* 2011; 26: 2004–10.
- Mosley PE, Breakspear M, Coyne T, Silburn P, Smith D. Caregiver burden and caregiver appraisal of psychiatric symptoms are not

- modulated by subthalamic deep brain stimulation for Parkinson's disease. *NPJ Parkinsons Dis* 2018a; 4: 12.
- Mosley PE, Smith D, Coyne T, Silburn P, Breakspear M, Perry A. The site of stimulation moderates neuropsychiatric symptoms after subthalamic deep brain stimulation for Parkinson's disease. *NeuroImage* 2018b; 18: 996–1006.
- Nambu A, Tokuno H, Takada M. Functional significance of the cortico-subthalamo-pallidal 'hyperdirect' pathway. *Neurosci Res* 2002; 43: 111–7.
- Nombela C, Rittman T, Robbins TW, Rowe JB. Multiple modes of impulsivity in Parkinson's disease. *PLoS One*; 2014 9: e85747.
- Obeso I, Wilkinson L, Casabona E, Bringas ML, Alvarez M, Alvarez L et al. Deficits in inhibitory control and conflict resolution on cognitive and motor tasks in Parkinson's disease. *Exp Brain Res* 2011; 212: 371–84.
- O'Callaghan C, Naismith SL, Hodges JR, Lewis SJ, Hornberger M. Fronto-striatal atrophy correlates of inhibitory dysfunction in Parkinson's disease versus behavioural variant frontotemporal dementia. *Cortex* 2013a; 49: 1833–43.
- O'Callaghan C, Naismith SL, Shine JM, Bertoux M, Lewis SJ, Hornberger M. A novel bedside task to tap inhibitory dysfunction and fronto-striatal atrophy in Parkinson's disease. *Parkinsonism Relat Disord* 2013b; 19: 827–30.
- O'Doherty JP, Deichmann R, Critchley HD, Dolan RJ. Neural responses during anticipation of a primary taste reward. *Neuron* 2002; 33: 815–26.
- Paliwal S, Mosley PE, Breakspear M, Coyne T, Silburn P, Aponte E, et al. Subjective estimates of uncertainty during gambling and impulsivity after subthalamic deep brain stimulation for Parkinson's disease. *Scientific Reports* 2019; doi: 10.1038/s41598-019-51164-2.
- Paliwal S, Petzschner FH, Schmitz AK, Tittgemeyer M, Stephan KE. A model-based analysis of impulsivity using a slot-machine gambling paradigm. *Front Hum Neurosci* 2014; 8: 428.
- Patton JH, Stanford MS, Barratt ES. Factor structure of the Barratt impulsiveness scale. *J Clin Psychol* 1995; 51: 768–74.
- Pauli WM, Nili AN, Tyszkla JM. A high-resolution probabilistic in vivo atlas of human subcortical brain nuclei. *Sci Data* 2018; 5: 180063.
- Peper JS, Mandl RC, Braams BR, de Water E, Heijboer AC, Koolschijn PC, et al. Delay discounting and frontostriatal fiber tracts: a combined DTI and MTR study on impulsive choices in healthy young adults. *Cereb Cortex* 2013; 23: 1695–702.
- Possin KL, Brambati SM, Rosen HJ, Johnson JK, Pa J, Weiner MW, et al. Rule violation errors are associated with right lateral prefrontal cortex atrophy in neurodegenerative disease. *J Int Neuropsychol Soc* 2009; 15: 354–64.
- Rae CL, Correia MM, Altena E, Hughes LE, Barker RA, Rowe JB. White matter pathology in Parkinson's disease: the effect of imaging protocol differences and relevance to executive function. *NeuroImage* 2012; 62: 1675–84.
- Rae CL, Hughes LE, Anderson MC, Rowe JB. The prefrontal cortex achieves inhibitory control by facilitating subcortical motor pathway connectivity. *J Neurosci* 2015; 35: 786–94.
- Raffelt D, Tournier JD, Rose S, Ridgway GR, Henderson R, Crozier S, et al. Apparent fibre density: a novel measure for the analysis of diffusion-weighted magnetic resonance images. *NeuroImage* 2012; 59: 3976–94.
- R Core Team. R: a language and environment for statistical computing. Vienna: R Foundation for Statistical Computing; 2014.
- Reise SP, Bonifay WE, Haviland MG. Scoring and modeling psychological measures in the presence of multidimensionality. *J Pers Assess* 2013; 95: 129–40.
- Robbins TW, Gillan CM, Smith DG, de Wit S, Ersche KD. Neurocognitive endophenotypes of impulsivity and compulsivity: towards dimensional psychiatry. *Trends Cogn Sci* 2012; 16: 81–91.
- Robinson GA, Cipolotti L, Walker DG, Biggs V, Bozzali M, Shallice T. Verbal suppression and strategy use: a role for the right lateral prefrontal cortex? *Brain* 2015; 138: 1084–96.
- Robinson G, Shallice T, Bozzali M, Cipolotti L. The differing roles of the frontal cortex in fluency tests. *Brain* 2012; 135: 2202–14.
- Rudebeck PH, Murray EA. The orbitofrontal oracle: cortical mechanisms for the prediction and evaluation of specific behavioral outcomes. *Neuron* 2014; 84: 1143–56.
- Sanchez G. PLS path modeling with R. Berkeley: Trowchez Editions; 2013.
- Schuepbach WM, Rau J, Knudsen K, Volkmann J, Krack P, Timmermann L, et al. Neurostimulation for Parkinson's disease with early motor complications. *N Engl J Med* 2013; 368: 610–22.
- Schultz W, Dayan P, Montague PR. A neural substrate of prediction and reward. *Science* 1997; 275: 1593–9.
- Seymour B, Barbe M, Dayan P, Shiner T, Dolan R, Fink GR. Deep brain stimulation of the subthalamic nucleus modulates sensitivity to decision outcome value in Parkinson's disease. *Sci Rep* 2016; 6: 32509.
- Shaw P, Weingart D, Bonner T, Watson B, Park MT, Sharp W, et al. Defining the neuroanatomic basis of motor coordination in children and its relationship with symptoms of attention-deficit/hyperactivity disorder. *Psychol Med* 2016; 46: 2363–73.
- Shores EA, Carstairs JR, Crawford JR. Excluded letter fluency test (ELF): norms and test-retest reliability data for healthy young adults. *Brain Impair* 2006; 7: 26–32.
- Smith SM, Jenkinson M, Woolrich MW, Beckmann CF, Behrens TE, Johansen-Berg H, et al. Advances in functional and structural MR image analysis and implementation as FSL. *NeuroImage* 2004; 23: S208–19.
- Smulders K, Esselink RA, Cools R, Bloem BR. Trait impulsivity is associated with the risk of falls in Parkinson's disease. *PLoS One* 2014; 9: e91190.
- Spiegel J, Hellwig D, Samnick S, Jost W, Mollers MO, Fassbender K, et al. Striatal FP-CIT uptake differs in the subtypes of early Parkinson's disease. *J Neural Transm* 2007; 114: 331–5.
- Stark AJ, Smith CT, Lin Y-C, Petersen KJ, Trujillo P, Van Wouwe NC, et al. Nigrostriatal and mesolimbic D2/3 receptor expression in Parkinson's disease patients with compulsive reward-driven behaviors. *J Neurosci* 2018; 38: 3230–9.
- Tanaka SC, Balleine BW, O'Doherty JP. Calculating consequences: brain systems that encode the causal effects of actions. *J Neuroscience* 2008; 28: 6750–5.
- Tournier JD, Calamante F, Connelly A. Robust determination of the fibre orientation distribution in diffusion MRI: non-negativity constrained super-resolved spherical deconvolution. *NeuroImage* 2007; 35: 1459–72.
- Tournier JD, Calamante F, Connelly A. Improved probabilistic streamlines tractography by 2nd order integration over fibre orientation distributions. *Proc Int Soc Magn Reson Med* 2010; 18: 1670.
- Tournier JD, Calamante F, Gadian DG, Connelly A. Direct estimation of the fiber orientation density function from diffusion-weighted MRI data using spherical deconvolution. *NeuroImage* 2004; 23: 1176–85.
- Tournier J-D, Smith RE, Raffelt DA, Tabbara R, Dhollander T, Pietsch M, et al. MRtrix3: A fast, flexible and open software framework for medical image processing and visualisation. *NeuroImage* 2019; 202. doi: 10.1016/j.neuroimage.2019.116137.
- van der Vegt JP, Hulme OJ, Zittel S, Madsen KH, Weiss MM, Buhmann C, et al. Attenuated neural response to gamble outcomes in drug-naive patients with Parkinson's disease. *Brain* 2013; 136: 1192–203.
- van Eimeren T, Pellecchia G, Cilia R, Ballanger B, Steeves TD, Houle S, et al. Drug-induced deactivation of inhibitory networks predicts pathological gambling in PD. *Neurology* 2010; 75: 1711–6.
- Vanegas-Arroyave N, Lauro PM, Huang L, Hallett M, Horowitz SG, Zaghoul KA, et al. Tractography patterns of subthalamic nucleus deep brain stimulation. *Brain* 2016; 139: 1200–10.
- Veraart J, Novikov DS, Christiaens D, Ades-Aron B, Sijbers J, Fieremans E. Denoising of diffusion MRI using random matrix theory. *NeuroImage* 2016; 142: 394–406.

- Vila M, Perier C, Feger J, Yelnik J, Faucheux B, Ruberg M, et al. Evolution of changes in neuronal activity in the subthalamic nucleus of rats with unilateral lesion of the substantia nigra assessed by metabolic and electrophysiological measurements. *Eur J Neurosci* 2000; 12: 337–44.
- Voon V, Gao J, Brezing C, Symmonds M, Ekanayake V, Fernandez H, et al. Dopamine agonists and risk: impulse control disorders in Parkinson's disease. *Brain* 2011; 134: 1438–46.
- Voon V, Pessiglione M, Brezing C, Gallea C, Fernandez HH, Dolan RJ, et al. Mechanisms underlying dopamine-mediated reward bias in compulsive behaviors. *Neuron* 2010a; 65: 135–42.
- Voon V, Reynolds B, Brezing C, Gallea C, Skaljic M, Ekanayake V, et al. Impulsive choice and response in dopamine agonist-related impulse control behaviors. *Psychopharmacology (Berlin)* 2010b; 207: 645–59.
- Weintraub D, Koester J, Potenza MN, Siderowf AD, Stacy M, Voon V, et al. Impulse control disorders in Parkinson disease: a cross-sectional study of 3090 patients. *Arch Neurol* 2010; 67: 589–95.
- Weintraub D, Mamikonyan E, Papay K, Shea JA, Xie SX, Siderowf A. Questionnaire for impulsive-compulsive disorders in Parkinson's Disease–Rating Scale. *Mov Disord* 2012; 27: 242–7.
- Wittmann BC, Daw ND, Seymour B, Dolan RJ. Striatal activity underlies novelty-based choice in humans. *Neuron* 2008; 58: 967–73.
- Xia M, Wang J, He Y. BrainNet viewer: a network visualization tool for human brain connectomics. *PLoS One* 2013; 8: e68910.
- Zhang Y, Brady M, Smith S. Segmentation of brain MR images through a hidden Markov random field model and the expectation-maximization algorithm. *IEEE Trans Med Imaging* 2001; 20: 45–57.